



Structural, Half-Metallic, Optical, and Thermoelectric Study on the Zr_2TiX ($X = Al, Ga, Ge, Si$) Heuslers: by DFT

Nosrat-Ali Vahabzadeh¹ · Arash Boochani² · Seyed Moammad Elahi³ · Hossein Akbari¹

Received: 16 January 2018 / Accepted: 22 June 2018 / Published online: 3 July 2018
© Springer Nature B.V. 2018

Abstract

Based on the density functional theory (DFT) framework, the mechanical, half-metallic (HF), optical and thermoelectric properties of Zr_2TiX ($X = Al, Ga, Ge, Si$) Heusler compounds are calculated. The mechanical calculations show good agreement of the lattice constant results with other experiment. The magnetic moments of Zr_2TiX ($X = Al, Ga, Ge, Si$) compounds have been calculated by 1.95, 1.85, 2 and $2.1\mu_B$ respectively and their stability were founded in the ferromagnetic phase for all cases. The density of states (DOS) indicates splitting states on Fermi level due to Zr d and Ti d overlapping by an asymmetry behavior at two dp and dn spins. The elastic stability, Paugh and Cauchy coefficients imply to the soft and ductility nature of these materials. Also, the optical parameters such as dielectric, refraction, absorption and loss functions have been shown the optical response in the visible area. The thermoelectric treatments indicate good electronic and thermal conductivity with high Seebeck and merit coefficient which is sensitive to the external magnetic moments.

Keywords Zr_2TiX ($X = Al, Ga, Ge, Si$) · Half-metallic · Optical properties · DFT

1 Introduction

The spin based transfer of electron is referred as spintronics [1–4], which is very interesting for the electronic industry in order to make magnetic read heads, giant magnetic resonance (GMR) [5], and tunneling magnetic resonance (TMR) [6–8]. The half-metals (HM) have very useful application in spintronic beside metallic and semiconductor behavior in majority and minority spins respectively, which are divided into two main classes, binary [9, 10] and Heusler compounds [11–13]. Heusler compounds are an important class of matters in the HM category, which are divided to two half- and full- heusler with high Curie temperature [14–17]. The full-heuslers with X_2YZ crystal lattice and L_{21} space group, where X and Y belong to transition metals

and Z is a III-Vth element of the periodic table. Also, some reports have shown a new crystal structure of heuslers named Li_2AgSb , which Y atom has more electronegativity than X [18–27]. Recently, the Zr based heuslers are taken into consideration theoretically and experimentally [28–34], whereas the Z and Y atomic positions are in (0, 0, 0) and (1/2, 1/2, 1/2) and X ones in (1/4, 1/4, 1/4) and (3/4, 3/4, 3/4) respectively, which show the HM nature and high magnetization; therefore, these compounds are good candidates for spintronic applications.

The thermoelectric (TE) phenomena is a way for conversion the temperature gradient to electrical current via Seebeck effect and vice versa, and it is even more attractive for improving thermal energy efficiency in heat recovery and cooling. The thermoelectric generators contribute to sustainability through scavenging of loss heat [35], which points that the TE treatment is a function of temperature. The 18-electron intermetallic systems Zr_2TiX ($X = Al, Ga, Ge, and Si$) might be good candidates for TE applications due to their high bulk modulus.

The spin polarization current is very interesting in the spintronic and TE industry, so spin depends on the TE phenomena lead to a contention about the interaction between spin, charge and heat current [36]. For example, it might be the Seebeck coefficient cause to a spin

✉ Arash Boochani
arash_bch@yahoo.com

¹ Department of Physics, Ardabil Branch, Islamic Azad University, Ardabil, Iran

² Department of Physics, Kermanshah Branch, Islamic Azad University, Kermanshah, Iran

³ Department of Physics, Faculty of Sciences, Science and Research Branch, Islamic Azad University, Tehran, Iran

accumulation by the thermal gradient [37]. This spin accumulation might lead to generate the spinning current in the thermoelectric devices [38]. The ferromagnetic Half-metals are the good candidate for the mentioned purposes due to their spin polarization at the Fermi level. Until now, the surface effects, interfaces, and defects are the main problems to generate the spin polarization currents in the Half-metal devices [39], so the theoretical investigations of novel thermoelectric devices being able to inject currents of high spin polarization are indeed important and being investigated -for instance- in Ref. [40].

In this paper, the structural, half-metallic, optical and thermoelectric properties in the two up and down spins of Zr_2TiX ($X = Al, Ga, Ge, Si$) compounds are calculated based on the FP-LAPW+lo method. Till now, the thermoelectric behavior of the mentioned cases has not been considered. Thus, the Computational methods are presented in Section 2, the results such as structural, HM, optical and thermoelectric treatments are discussed in Section 3, and finally, the conclusion is present in Section 4.

2 Computational Methods

The structural, half-metallic, optical and thermoelectric treatment of Zr_2TiX ($X = Al, Ga, Ge, Si$) compounds was carried out based on the density functional theory (DFT) framework by FP-LAPW+lo method [41] using Wien2K and BoltzTraP codes [42, 43]. The exchange-correlation potential was approximated by GGA [44], also the optical calculations are approximated to RPA [45]. The optimized input parameters such as Rkmax, Kpoint and lmax were selected to 8.5, 20000 and 10 respectively. Also, other parameters such as muffin-tin spheres radii, separation energy and convergence in charges have been selected to 2.0(Bohr), -6.0 (Reyd) and 0.0001 respectively.

3 Results

3.1 Structural Properties

The unit cell volume changes versus energy (E-V) diagram contains important information about crystal properties such as lattice constant, equilibrium volume, bulk modulus and its derivative [46]. The E-V curves of the Zr_2TiX ($X = Al, Ga, Ge, Si$) compounds in the paramagnetic (PM) and ferromagnetic (FM) phases and their results were displayed in Fig. 1 and Table 1, respectively. Moreover, the structural characters of Zr_2CoAl , Zr_2CoGa , Zr_2CrGa and Zr_2CrAl compounds added to Table 1 for comparison with our compounds [47]. Figure 1 indicates that the FM phase is more stable than PM phase in all mentioned cases and by

applying the hydrostatic pressure a transition phase were occurred of FM to PM phase.

The elastic constants and its depended coefficients such as Debay temperature, Anisotropy coefficient, Young and Bulk modulus, Poisons ratio are important tools for better knowledge about the mechanical treatment of the matters. The study of elastic constants details is shown the mechanical natural of crystals such as stability and lattice hardness [48]. Based on the cubic symmetry of Zr_2TiX ($X = Al, Ga, Ge, Si$) compounds, only three C_{11} , C_{12} and C_{44} coefficients of the elastic tensor are non-zero. The Shear (G) and Bulk (B) modulus are related to the elastic constants based on the following equations:

$$B = 1/2(B_R + B_V) \quad G = 1/2(G_V + G_R) \quad (1)$$

Where, B_R , B_V , G_V , G_R are defined as follows:

$$B_R = B_V = \frac{C_{11} + 2C_{12}}{3} \quad (2)$$

$$G_V = \left(\frac{C_{11} - C_{12} + 3C_{44}}{5} \right) \quad (3)$$

$$G_R = \frac{5C_{44} (C_{11} - C_{12})}{[4C_{44} + 3(C_{11} - C_{12})]} \quad (4)$$

Also, Young modulus (E), Poison ratio (ν) and Anisotropy coefficient are based on the following equations:

$$E = \frac{9GB}{3B + G} \quad (5)$$

$$\nu = \frac{3B - 2G}{2(3B + G)} \quad (6)$$

$$A = \frac{2C_{44}}{(C_{11} - C_{12})} \quad (7)$$

One of the important scales for indicating the elastic stability in the cubic structure is [51]:

$$C_{11} - C_{12} > 0, C_{11} + 2C_{12} > 0, C_{44} > 0 \quad (8)$$

The elastic results are listed in Table 2 and it is clear that the all mentioned compounds have elastic stability. Another parameter for showing the characteristic of the angle of bonds is named the Cauchy pressure [52], which is calculated for all mentioned cases. This pressure is negative for non-metallic compounds and is positive for other cases, so, the metallic treatment of our compositions is confirmed. Moreover, the positive value of the Cauchy pressure indicates the soft nature and malleable of the Zr_2TiX ($X = Al, Ga, Ge, Si$) compounds. The Paugh relation which is defined by B/G [53], is another useful parameter for indicating the ductility or brittleness with $\frac{B}{G} > 1.75$ and $\frac{B}{G} < 1.75$ respectively, that Table 2 indicates the ductile behavior of our compounds. The Poisson's ratio is a parameter for indicate the nature bonds [54], so that the lower amount of this parameter implies the covalence bonds

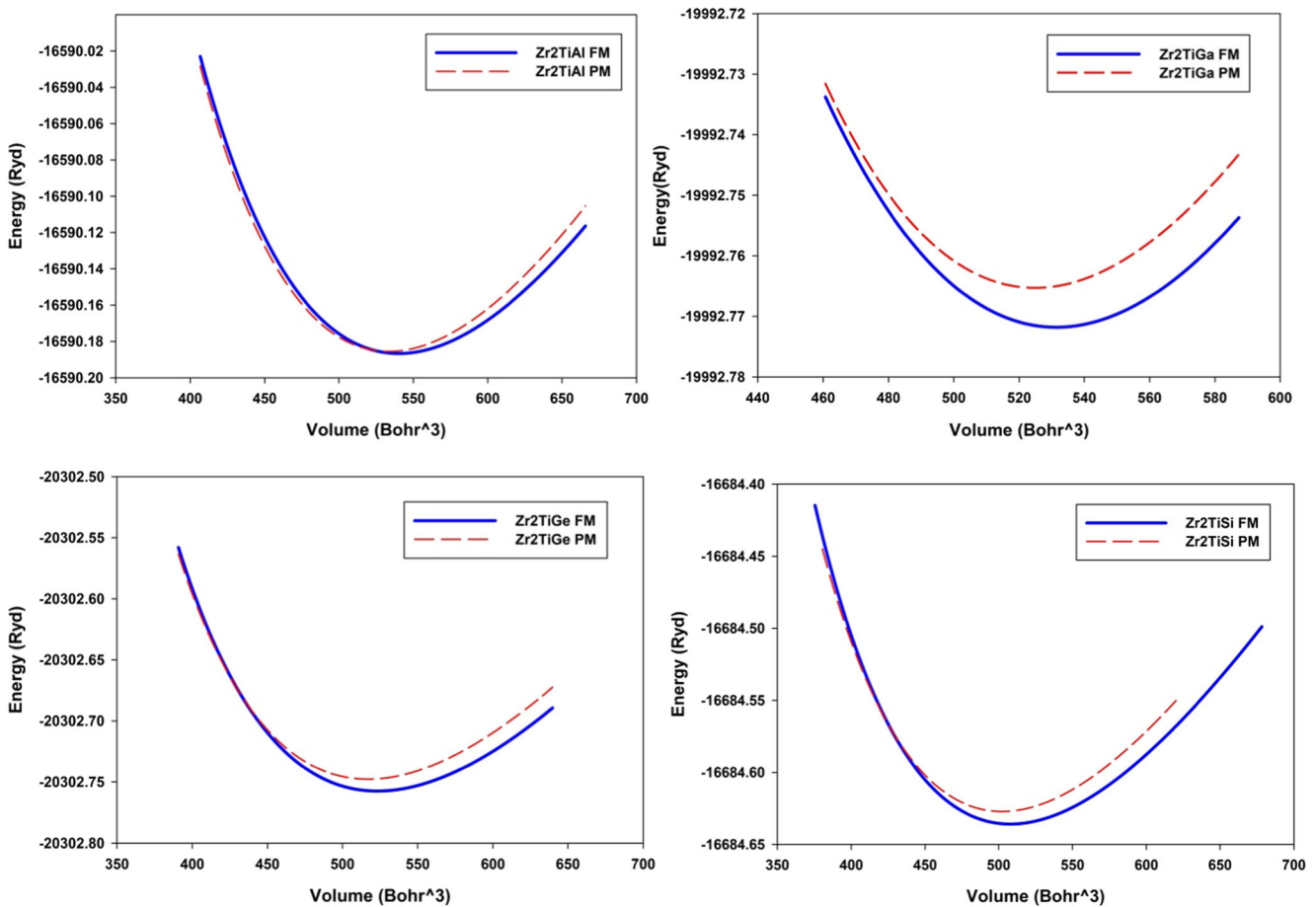


Fig. 1 The Energy-Volume (E-V) diagrams of Zr_2TiX ($X = Al, Ga, Ge, Si$) compounds in the Ferromagnetic (FM) and Paramagnetic (PM) phases

($\nu = 0.1$), while $\nu = 0.25$ represents ionic bonds and the amount between 0.25 to 0.5 represent central forces [55]. Our results in Table 2 confirm the central force bonds for

Table 1 The lattice constants, total magnetic moments, Bulk modulus and its derivative of the Zr_2TiX ($X = Al, Ga, Ge, Si$) compounds in the FM and PM phases

Compounds	a(A)	B(GPa)	B'	MMT (μ_B)
Zr_2TiAl (FM)	6.81	101.249	3.509	1.95
Zr_2TiAl (PM)	6.84 ^a			
Zr_2TiGa (FM)	6.75	102.713	3.701	1.87
Zr_2TiGa (PM)	6.77	104.629	4.117	
Zr_2TiGe (FM)	6.73	106.246	3.887	1.88
Zr_2TiGe (PM)	6.74	107.367	4.043	
Zr_2TiSi (FM)	6.67	111.290	3.832	1.87
Zr_2TiSi (PM)	6.68	113.786	3.832	
Zr_2CoAl	6.57	111.5	2.35	2.000 ^{a,b}
Zr_2CrAl	6.59	86.0	6.99	1.000 ^c
Zr_2CoGa	6.59	114.9	1.00	2.000 ^a
Zr_2CrGa	6.62	79.3	6.24	1.000 ^c

^{a,b,c}Ref [48–50]

Zr_2TiX ($X = Al, Ga, Ge, Si$) compounds. The anisotropy coefficient (A) shows the degree of elastic anisotropy [56], so that for isotropic matters $A = 1$, and deviation from A demonstrate the degree of elastic anisotropy. The A results have been implied to the elastic anisotropy nature of the mentioned compounds in Table 2.

3.2 Electronic Properties

The band levels graph versus symmetry directions in the first Brillion zone is named Band structure which contains the important information about electronic, optical and thermoelectric properties. The Band structures of Zr_2TiX ($X = Al, Ga, Ge, Si$) compounds were shown in Fig. 2 for up and down spins. In the -6 to -9 eV energy range, a level of 1s orbital belongs to $X = Al, Ga, Ge, Si$ atoms is presented which is located in the semi-core zone and will not contribute in conducting. The Fermi level of all cases has been cut off by levels in two spins and the metallic behavior appear in the mentioned spins. By a comparison between Fig. 2 curves, it is shown that the curve slop of Zr_2TiGe & Si compounds are higher than two others in Γ point so the electron mobility of these compounds are higher than

Table 2 The elastic constants and other related parameters: Bulk (B), Shear (G) and Yung (E) modules, the B/G relation, Poisson ratio (ν) and Anisotropy parameter (A)

Compounds	C_{11} (GPa)	C_{12} (GPa)	C_{44} (GPa)	$C_{12} - C_{44}$ (GPa)	B (GPa)	G (GPa)	E (GPa)	$\frac{B}{G}$	ν	A
Zr ₂ TiAl	119.414	92.167	64.186	27.981	101.249	43.961	115.209	2.330	0.310	4.711
Zr ₂ TiGa	115.144	99.090	58.544	40.546	104.441	38.331	102.458	2.724	0.336	7.239
Zr ₂ TiGe	141.290	106.424	58.670	82.621	118.046	42.175	113.060	2.798	0.340	3.365
Zr ₂ TiSi	147.560	113.063	61.231	51.832	123.562	43.638	117.125	2.832	0.342	3.549

two other compounds and the electronic, optical and thermal conductivity are too large.

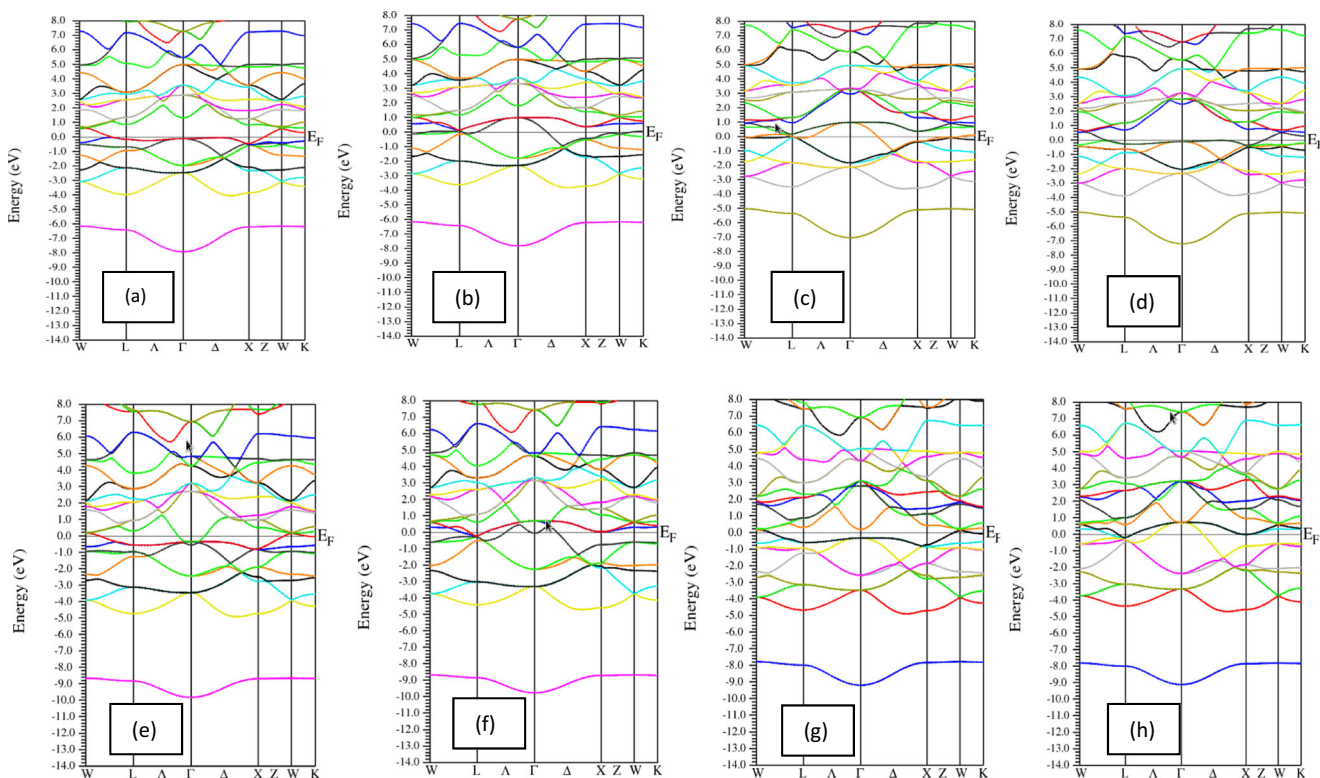
According to distinct electronic behaviors of the mentioned cases at two up and down spins, these compositions have the magnetic nature and the total magnetic moments are listed in Table 1, which are originated from Zr and Ti elements, which have a half empty d orbital. Our results show the magnetic moments based on GGA completely compatible with Slater Pauli rule:

$$m_t = N_v - 18\mu_B \quad (9)$$

Where N_v represent the valance band electron numbers.

The density of states (DOS) diagrams are depicted in Fig. 3 for up and down spins, which include the important information about the electronic and optical nature of matters. The different behavior of DOS at up and down spins confirms the magnetic nature of the compound

Figure 3 shows that Al, Ga Ge and Si states are located below the Fermi level and the Zr and Ti d orbitals are in Fermi level. Also, the Ti states have big peaks in two spins and its peaks are smaller for Zr. The $d - d$ of Zr-Ti and $p - d$ of Ti-X and Zr-X hybridization caused the spin split and spin polarization at Fermi level.

**Fig. 2** The Band structure of **a, b** Zr₂TiAl, **c, d** Zr₂TiGa, **e, f** Zr₂TiGe and **g, h** Zr₂TiSi at up and down spins, respectively

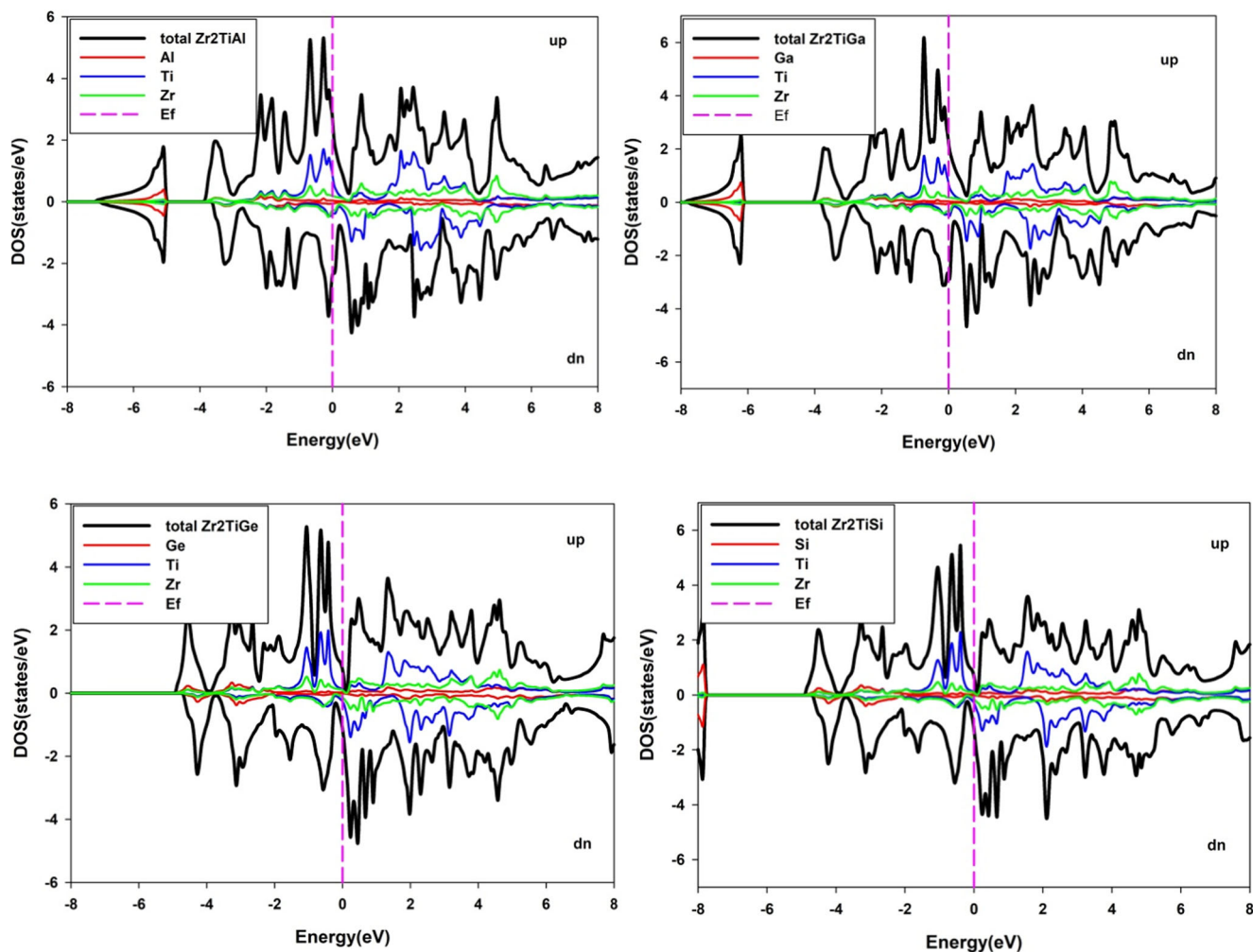


Fig. 3 The DOS curves of the Zr_2TiX ($X = Al, Ga, Ge, Si$) compounds at the up and down spins

3.3 Optical Properties

The matter response to incident light is named dielectric coefficient which divided into two real and imaginary parts. These coefficients are functions of the optical frequency and are characterized by the relation [57]:

$$\varepsilon(\omega) = \varepsilon_1(\omega) + i\varepsilon_2(\omega) \quad (10)$$

The real part of the dielectric function ($\varepsilon_1(\omega)$) for Zr_2TiX ($X = Al, Ga, Ge, Si$) compounds is depicted in Fig. 4a. It is shown that the static amount ($\varepsilon_1(\omega)$) of all cases tend to $-\infty$ which indicate the metallic nature of the these compounds Other than the visible area and the infrared edge, the $\varepsilon_1(\omega)$ sign is negative in all photon energies and Zr_2TiGa

has a much more response to incident light. Plasmonic oscillations occur when the $\varepsilon_1(\omega)$ and energy loss function (ELF) are zero and the maximum amounts, so comparing Fig. 4a and c is shown that the plasmonic frequencies are occurred in 17.5 eV, 19.5 eV for Zr_2TiAl , 20 eV for Zr_2TiGa and 21 eV for Zr_2TiGe and Si which implied to no losing light in the infrared, visible and ultra violet areas.

The matter response to the incident light in energy space is represented by the imaginary part of the dielectric function ($\varepsilon_2(\omega)$), so that its peaks indicate the electron transmission from the occupied to unoccupied levels. Based on the metallic nature of the mentioned compound, the static value of $\varepsilon_2(\omega)$ (Fig. 4b) has infinite values that indicate the intraband transitions, and by increasing photon energy, the $\varepsilon_2(\omega)$ peaks tend to the lower amounts, and after 15 eV become zero. The absorption curves are

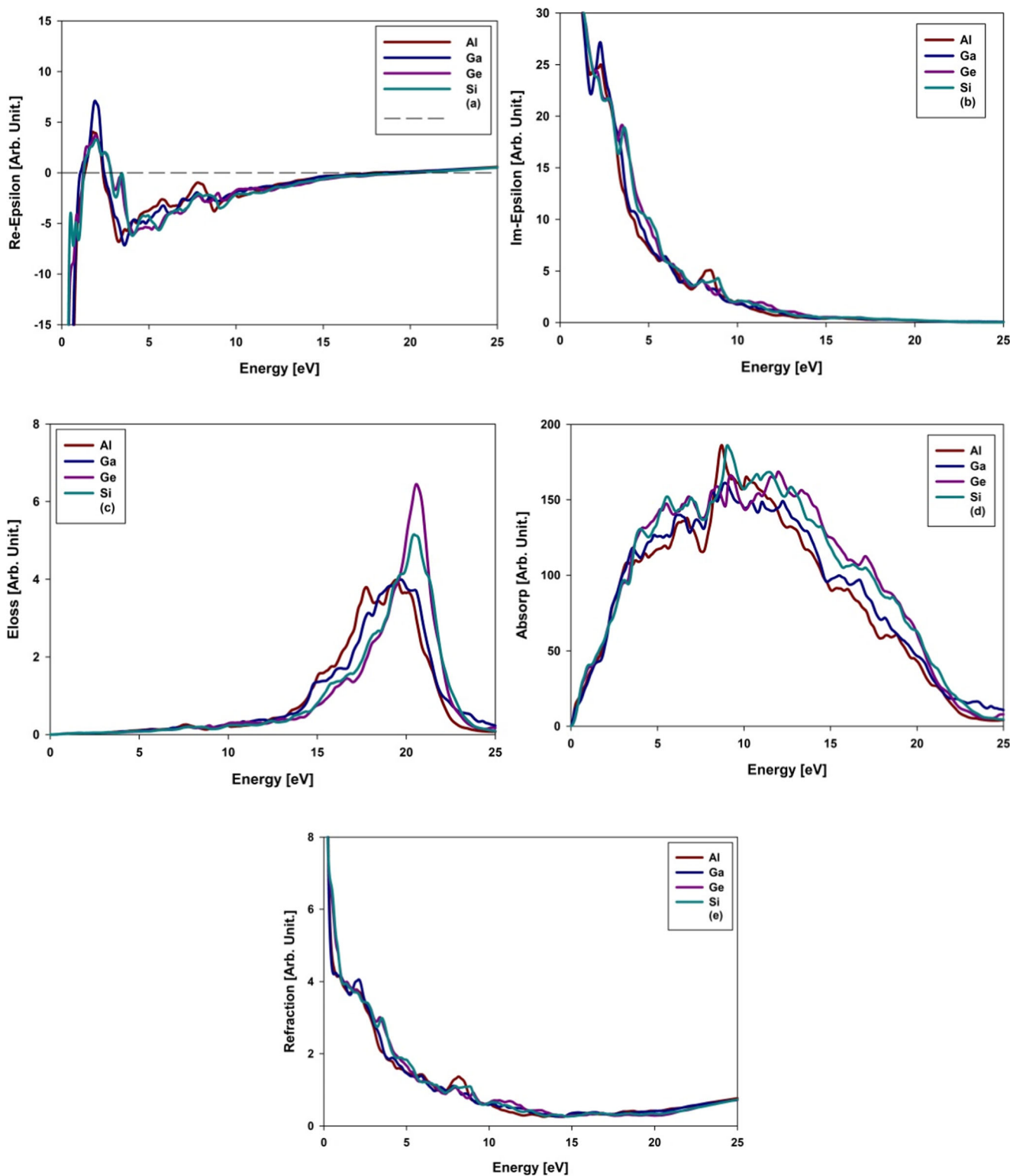


Fig. 4 The optical index of Zr_2TiX (X = Al, Ga, Ge, Si) compounds versus photon energy **a** $\epsilon_1(\omega)$, **b** $\epsilon_2(\omega)$, **c** ELF, **d** Absorption and **e** Refraction

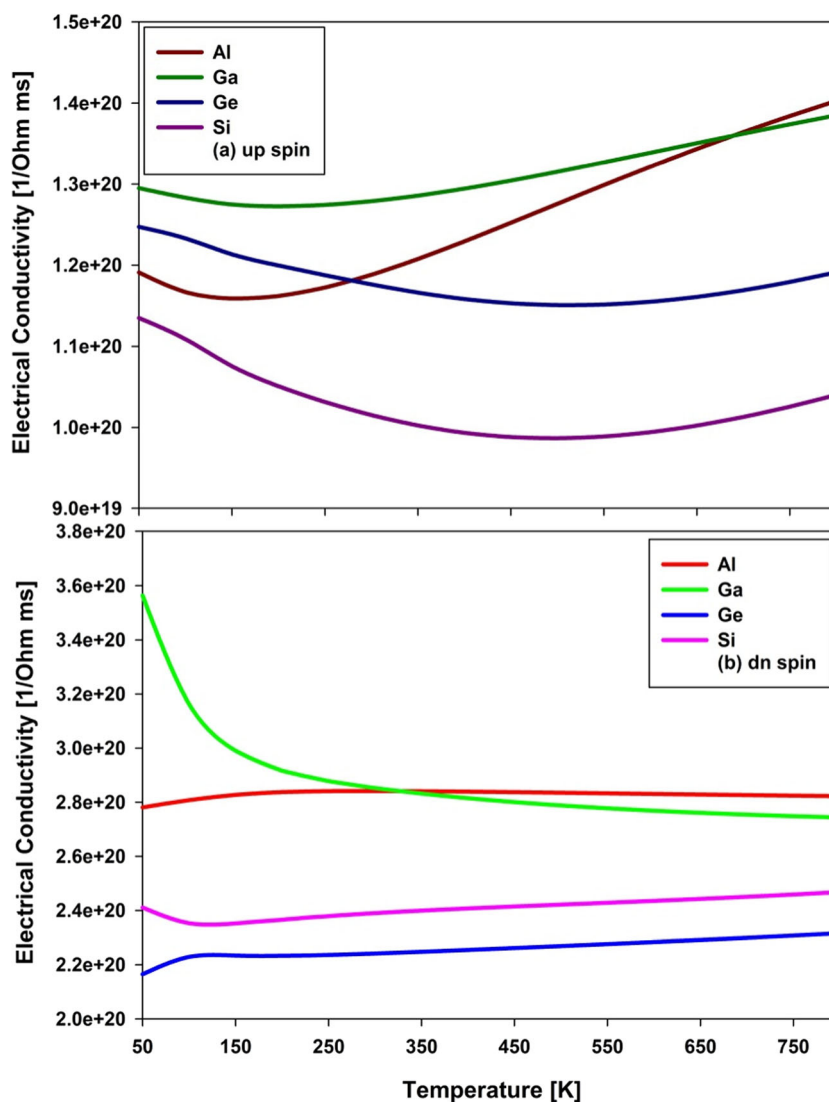
depicted in Fig. 4d which indicate increasing absorption in the visible area that are matched by $\epsilon_2(\omega)$ diagrams, so it can be said that the absorption in the mentioned

area belongs to optical transmissions, but the absorptions are increased by photon energy and reaches to maximum amounts in the 10 eV (UV area), on the other hand, $\epsilon_2(\omega)$

has a lower amount for every compound. The refractions are low too in the abovementioned energy ranges, so the mentioned compounds have transparent behavior. The refraction indices of Fig. 4e show big amounts of $n(0)$ confirming the metallic nature of these compounds, and after 10 eV are lower than one ($n(\omega) < 1$) indicating the superluminal phenomenon.

By a comparison between the ELF and $\varepsilon_1(\omega)$ curves, it is clear that the photon energy loss in the lower energies (IR, visible area and UV edge) are very low, so, these Heusler compounds are good candidates for optical applications in the mentioned energy. The ELF main peaks are occurred in 20 eV, wherever the $\varepsilon_1(\omega)$ diagrams are zero, which indicates the plasmonic frequencies. Of course the $\varepsilon_1(\omega)$ roots in the lower photon energies are related to refractions and reflections.

Fig. 5 The electrical conductivity (δ) of the Zr_2TiX ($X = Al, Ga, Ge, Si$) compounds in the **a** up, **b** down spins



3.4 Thermoelectric Properties

The thermoelectric behavior of the matter is strongly related to the Seebeck coefficient (S) and other thermoelectric parameters such as electronic (δ) and thermal (K) conductivities for isotropic electronic structure. In good thermoelectric materials, we should have: (a) the narrow energy gap, (b) the bands overlap in the edge of energy gap [58] and (c) the bands density near the Fermi level (E_f) [59, 60]. Another dimensionless thermoelectric coefficient is named thermoelectric efficiency or merit parameter as follows:

$$ZT = \frac{S^2 \delta T}{K} \quad (11)$$

which is related to S , δ , temperature (T) and K .

The electrical conductivity versus temperature for Zr_2TiX ($X = Al, Ga, Ge, Si$) compounds is depicted in Fig. 5 for the up and dn spins. Based on the high bands density in the Fermi edge and the metallic behavior of the mentioned cases, the good electronic conductivity at two up and dn spins are expected. In the temperatures (about 50 K), the electronic conductivity at dn spin is almost three times upper than the up spin. In $Zr_2Ti(Al \& Ga)$ cases, with increasing temperature after a downtrend in the thermal conductivity at up spin, it is heavily increased until 800 K, but in $Zr_2Ti(Ge \& Si)$ cases it is decreased. The electronic conductivity of Zr_2TiGe compound in dn spin at 50 K has the maximum amount, and after room temperature attains

the saturation limit, even that in the other three compounds in the range of 50 K to 800 K, it has a constant amount.

The total thermal conductivity of the matter belongs to the electron conductivity and lattice vibration, but based on the metallic nature of the mentioned cases, the electronic portion is more than lattice vibration ones. The thermal conductivities of the mentioned compounds are increased by applying temperature relatively linear in the dn and up spins, respectively, which indicate that the electronic carrier is higher in the high temperature than the lower one (Fig. 6).

The S coefficients of the Zr_2TiX ($X = Al, Ga, Ge, Si$) compounds are shown in the Fig. 7. This parameter is a sensitive tool for testing the electronic structure of

Fig. 6 The thermal conductivity (K) of the Zr_2TiX ($X = Al, Ga, Ge, Si$) compounds in the **a** up, **b** down spins

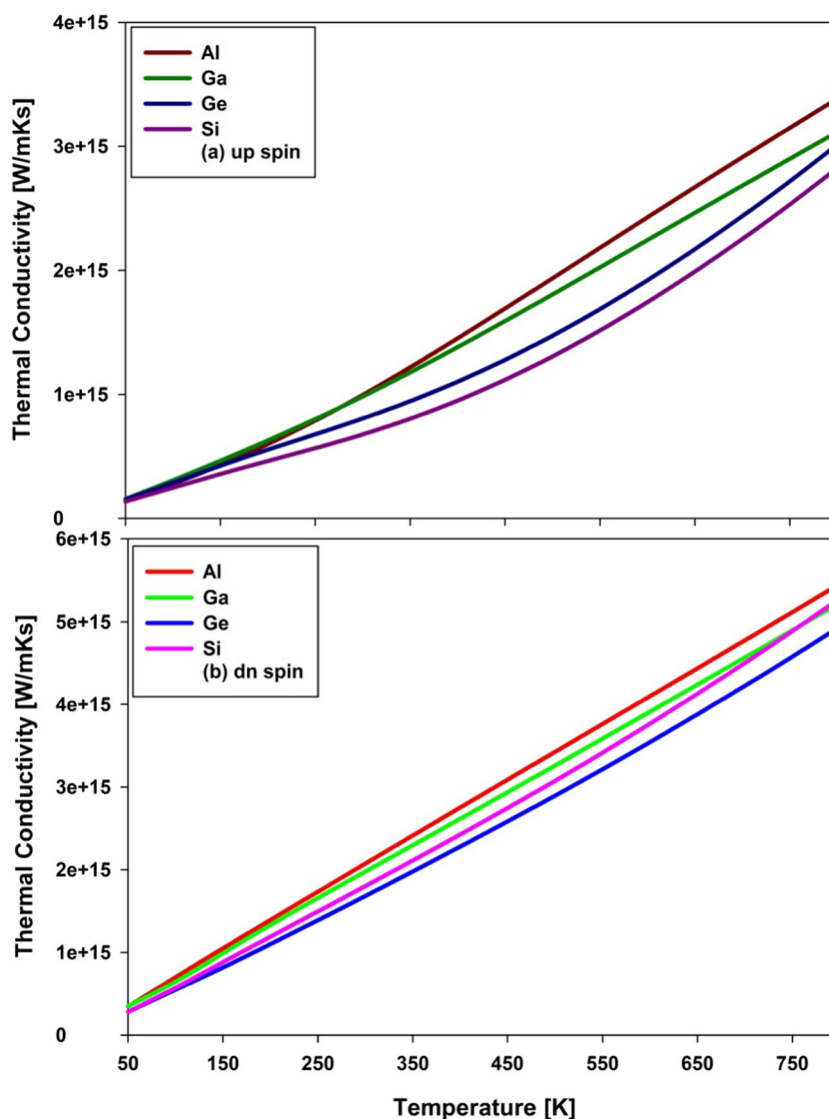
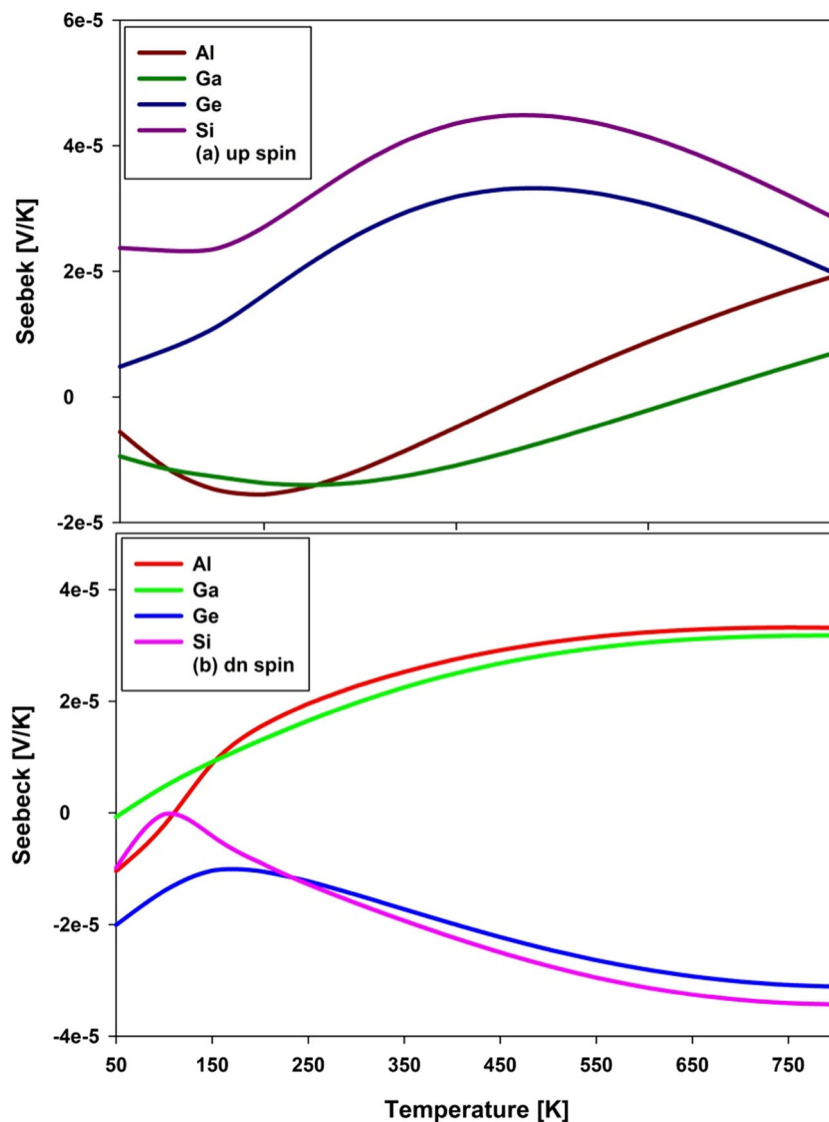


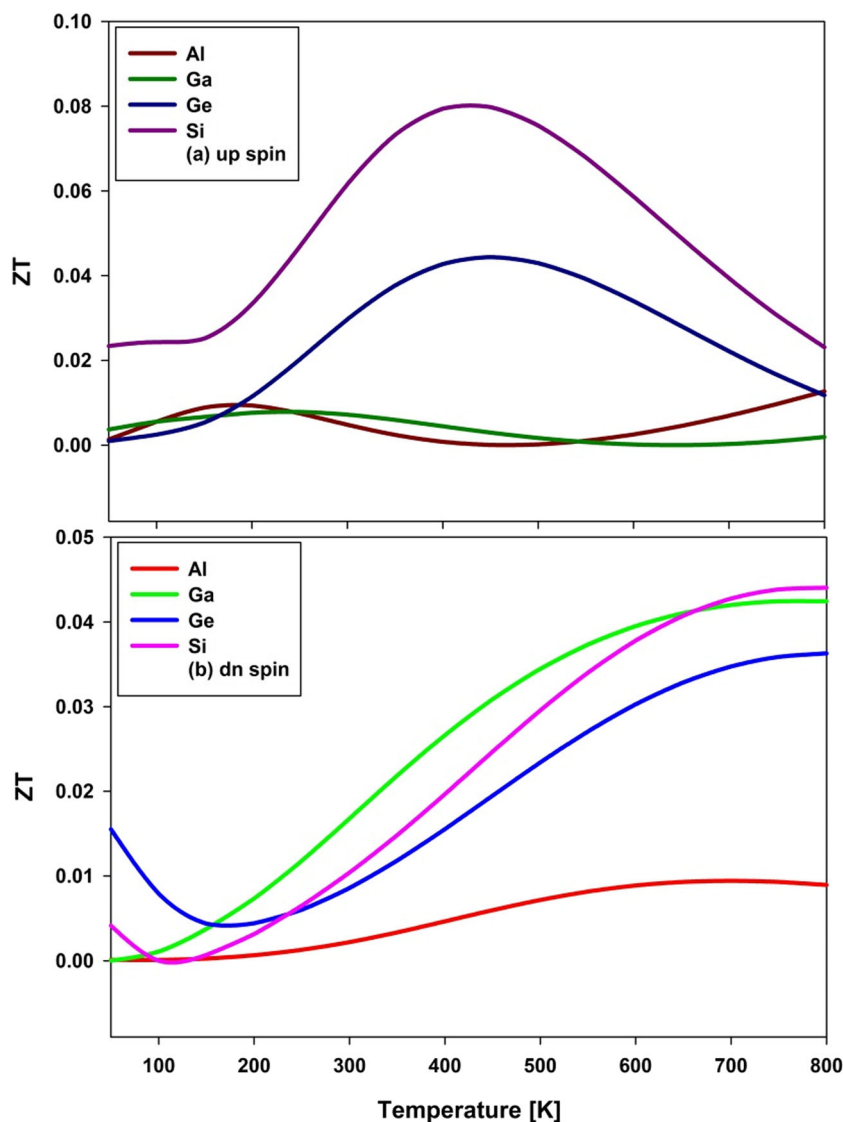
Fig. 7 Seebeck coefficients (S) of the Zr_2TiX ($X = Al, Ga, Ge, Si$) compounds in the **a** up, **b** down spins



matters, which has the order of magnitude $\mu V K^{-1}$ for metals and is relatively big for semiconductors. The S parameters of the mentioned half metallic compounds are depicted, and it is shown that by increasing temperature the deeper electronic levels are contributed in the electronic conduction. The S sign of $Zr_2Ti(Ge, Si)$ is positive and for $Zr_2Ti(Al, Ga)$ is negative until 650 K in the up spin. By increasing temperature until room temperature, the S coefficient of $Zr_2Ti(G, Si)$ compounds have been changed and after that, it has been reduced slowly. In the two other cases, the S parameters are decreased by increasing temperature until 250 K, and after this, it has a linear treatment. But the S sign in the dn spin is changed for the mentioned cases than up spin, so that $Zr_2Ti(Al, Ga)$ and

$Zr_2Ti(Ge, Si)$ have positive and negative sign respectively, and by increasing temperature the S coefficient attain a saturation limit. The negative sign of S is implied to the n-type nature of the charge carriers. The figure of merit (ZT) is an important dimensionless parameter to indicate the electrical and optical conductivity quality. The ZT has a big amount for good thermoelectric matters. Figure 8 shows the ZT of the mentioned cases in up and dn spins at the range of 50 K to 800K. The ZT amount of the $Zr_2Ti(Al, Ga)$ is a small amount but for $Zr_2Ti(Ge, Si)$ compounds, it is rapidly increased by increasing temperature until 50 K, and then it is decreased in the up spin. But in the dn spin, the Zr_2TiAl has a small value while in the three other cases, the ZT are increased linearly and in the 700 K is reached to a saturation limit.

Fig. 8 The figure of merit (ZT) of the Zr_2TiX ($X = Al, Ga, Ge, Si$) compounds in the **a** up, **b** down spins



4 Conclusions

In summary, the elastic, HM, optical and thermoelectric properties of Zr_2TiX ($X = Al, Ga, Ge, Si$) Heusler compounds were calculated by DFT within the GGA. From the mechanical computations, the E-V diagrams indicate more stability in the FM phase than in NM one, and the elastic parameters of these compounds implied to the ductility behavior. There is a central force in the mentioned compounds by anisotropy elastic nature. The DOS and Band structure diagrams indicate the magnetic treatment of these compounds with good metallic behavior at both spins. The optical responses to the incident light occur in lower photon energies that imply the metallic nature of the mentioned cases. The ELF peaks are located in higher energies and plasmonic frequencies are in the UV region.

The covalence and ionic bonds with metallic behavior in the two up and down spins of these compounds were made

a good base for thermoelectric applications. Our results indicate high electrical and thermal conductivity in the two spins and the Seebeck and ZT coefficients parameters are increased in the room temperature.

References

1. Prinz GA (1995) *Phys Today* 48:58
2. Kobayashi KI, Kimura T, Sawada H, Terakura K, Tokura K (1998) *Nature* 395:677
3. Park JH, Vescovo E, Kim HJ, Kwon C, Ramech R, Venkatesan T (1998) *Nature* 392:794
4. Hashemifar SJ, Kratzer P, Scheffler M (2005) *Phys Rev Lett* 94:096402
5. Felser T, Graf C, Parkin SSP (2011) *Prog Solid State Chem* 39:1
6. Mavropoulos P, Lezaic M, Blugel S (2005) *Phys Rev B* 72:174428
7. Lezaic M, Mavropoulos PH, Enkovaara J, Bihlmayer G, Bluge S (2006) *Phys Rev Lett* 97:026404

8. Chadov S, Graf T, Chadova K, Dai X, Casper F, Fecher GH, Felser C (2011) *Phys Lett* 107:47202
9. Boochani A, Abolhasani MR, Ghoranneviss M, Elahi M (2010) *Commun Theor Phys* 54:148
10. Rezaee S, Boochani A, Majidiyan M, Ghaderi A, Solaymani S, Naseri M (2014) *Rare Met* 33:615–621
11. Boochani A, Khosravi H, Khodadadi J, Solaymani S, Sarmazdeh MM, Mendi RT, Elahi SM (2015) *Commun Theor Phys* 63:641
12. Ahmadian F, Boochani A (2011) *Physica B* 406:2865–2870
13. Boochani A, Nowrozi B, Khodadadi J, Solaymani S, Jalali-Asadabadi S (2017) *J Phys Chem C* 121:3978–3986
14. de Groot RA, Mueller FM, van Engen PG, Buschow KHJ (1983) *Phys Rev Lett* 50:2024
15. Zutic I, Fabian J, Das Sarma S (2004) *Rev Mod Phys* 76:323
16. Zenasni HH, Faraoun I, Esling C (2013) *J Magn Magn Mater* 333:162
17. Casper F, Graf T, Chadov S, Balke B, Felser C (2012) *Semicond Sci Technol* 27:10172
18. Liu GD, Dai XF, Yu SY, Zhu ZY, Chen JL, Wu GH, Zhu H, Xiaob JQ (2006) *Phys Rev B* 74:054435
19. Wei XP, Chu SB, Mao GY, Deng H, Lei T, Hu XR (2011) *J Magn Mater* 323:2295
20. Liu GD, Dai X, Liu HY, Lhen JL, Li YX (2008) *Phys Rev B* 77:014424
21. Bayar E, Kervan N, Kervan S (2011) *J Magn Mater* 323:2945
22. Fang QL, Zhang JM, Xu KW, Ji V (2013) *J Magn Mater* 345:171
23. Kervan N, Kervan S, Magn J (2012) *Magn Mater* 324:645
24. Wei XP, Deng JB, Mao GY, Chu SB, Hu XR (2012) *Intermetallics* 299:86
25. Jia HY, Dai X, Wang LY, Liu R, Wang XT, Li PP, Cui YYT, Liu GD, Magn J (2014) *Magn Mater* 367:33
26. Birsan A, Palade P, Kuncser V (2013) *J Magn Magn* 331:109
27. Ahmadian F, Salary A (2014) *Intermetallics* 46:243
28. Wang XT, Cui YT, Liu XF, Liu GD (2015) *J Magn Magn Mater* 394:50
29. Birsan A (2014) *Curr Appl Phys* 14:1434
30. Deng Z-Y, Zhang J-M (2016) *J Magn Magn Mater* 397:120
31. Deng Z-Y, Zhang J-M (2016) *J Magn Magn Mater* 409:28
32. Gao YC, Wang XT, Rozale H, Lu JW (2015) *J Kor Phys Soc* 67:881
33. Wang XT, Lin TT, Rozale HH, Dai X, Liu GD (2016) *J Magn Magn Mater* 402:190
34. Alijani V, Winterlik J, Fecher GH, Naghavi SS, Felser C (2011) *Phys Rev B* 83:184428
35. Snyder GJ, Toberer ES (2008) Complex thermoelectric materials. *Nat Mater* 7:105–114
36. Bauer GEW, Saitoh E, van Wees BJ (2012) *Nat Mater* 11:391
37. Slachter A, Bakker FL, Adam J-P, van Wees BJ (2010) *Nat Phys* 6:879
38. Chadov S, Graf T, Chadova K, Dai X, Casper F, Fecher GH, Felser C (2011) *Phys Rev Lett* 107:047202
39. Katsnelson MI, Irkhin VY, Chioncel L, Lichtenstein AI, de Groot RA (2008) *Rev Mod Phys* 80:315
40. Chadov S, Graf T, Chadova K, Dai X, Casper F, Fecher GH, Felser C (2011) *Phys Rev Lett* 107:047202
41. Slater JC (1964) *Adv Quant Chem* 1:5564
42. Madsen GKH, Singh DJ (2006) BoltzTrap: a code for calculating band-structure dependent quantities. *Comput Phys Commun* 175:67–71
43. Blaha P, Schwarz K, Madsen GKH, Kvasnicka D, Luitz J (2001) WIEN2K, an augmented plane wave + local orbitals program for calculating crystal properties 3-9501031-1-2, Karlheinz Schwarz, Technische Universität, Wien
44. Perdew JP, Burke K, Ernzerhof M (1996) *Phys Rev Lett* 77:3865
45. Ren X, Rinke P, Joas C, Scheffler M (2012) *J Mater Sci* 47:7447
46. Murnaghan FD (1944) *Proc Natl Acad Sci USA* 30:244
47. Wei X-P, Zhang Y-L, Wang T, Sun X-W, Song T, Guo P, Deng J-B (2017) *Mater Res Bull* 86:139–145
48. Wang JY, Zhou YC (2004) *Phys Rev B* 69:214111–214119
49. Birsan A (2014) *Curr Appl Phys* 14:1434
50. Deng Z-Y, Zhang J-M (2016) *J Magn Mater* 397:120
51. Pettiifor DG (1992) *J Mater Sci Technol* 8:345–349
52. Liu Y, Hu W-C, Li D-J, Zeng X-Q, Xu C-S, Yang X-J (2012) *Intermetallics* 31:257–263
53. Rahman MD, Rahaman MD (2015) The structural, elastic, electronic and optical properties of MgCu under pressure: a first-principles study arXiv preprint arXiv:1510.02020
54. Pfrommer BG, Côté M, Louie SG, Cohen ML (1997) *J Comput Phys* 131:233
55. Zener C (1948) *Elasticity and anelasticity of metals*. University of Chicago Press, Chicago
56. *Materials studio castep manual*. Accelrys (2010) 261–262
57. Hossain MA, Ali MS, Islam AKMA (2012) *Eur Phys J B* 85:396. <https://doi.org/10.1140/ejpb/e2012-30799>
58. Kondo T, Takeuchi T, Tsuda S, Shin S (2006) *Phys Rev B* 74:224511
59. Shankar A, Rai DP, Khenata R, Maibam J, Sandeep, Thapa RK (2015) *J Alloys Compd* 619:621–626
60. Heremans JP, Jovovic V, Toberer ES, Saramat A, Kurosaki K, Charoenphakdee A, Yamanaka S, Snyder GJ (2008) *Science* 321:554